EUROPEAN ORGANIZATION FOR NUCLEAR RESEARCH

CERN-PH-EP/2007-023
09 July 2007

Charged-Particle Multiplicities in Charged-Current Neutrino– and Anti-Neutrino–Nucleus Interactions

CHORUS Collaboration

Abstract

The CHORUS experiment, designed to search for $\nu_\mu \rightarrow \nu_\tau$ oscillations, consists of a nuclear emulsion target and electronic detectors. In this paper, results on the production of charged particles in a small sample of charged-current neutrino– and anti-neutrino–nucleus interactions at high energy are presented. For each event, the emission angle and the ionization features of the charged particles produced in the interaction are recorded, while the standard kinematic variables are reconstructed using the electronic detectors. The average multiplicities for charged tracks, the pseudo-rapidity distributions, the dispersion in the multiplicity of charged particles and the KNO scaling are studied in different kinematical regions. A study of quasi-elastic topologies performed for the first time in nuclear emulsions is also reported. The results are presented in a form suitable for use in the validation of Monte Carlo generators of neutrino–nucleus interactions.

To be published in European Physical Journal C

CHORUS Collaboration

A. Kayis-Topaksu, G. Önengüt
Çukurova University, Adana, Turkey
R. van Dantzig, M. de Jong, R.G.C. Oldeman[1]
NIKHEF, Amsterdam, The Netherlands
M. Güler, U. Köse, P. Tolun
METU, Ankara, Turkey
M.G. Catanesi, M.T. Muciaccia
Università di Bari and INFN, Bari, Italy
K. Winter
Humboldt Universität, Berlin, Germany[2]
B. Van de Vyver[3,4], P. Vilain[5], G. Wilquet[5]
Inter-University Institute for High Energies (ULB-VUB) Brussels, Belgium
B. Saitta
Università di Cagliari and INFN, Cagliari, Italy
E. Di Capua
Università di Ferrara and INFN, Ferrara, Italy
S. Ogawa, H. Shibuya
Toho University, Funabashi, Japan
I.R. Hristova[6], T. Kawamura, D. Kolev[7], H. Meinhard, J. Panman, A. Rozanov[8], R. Tsenov[7], J.W.E. Uiterwijk, P. Zucchelli[3,9]
CERN, Geneva, Switzerland
J. Goldberg
Technion, Haifa, Israel
M. Chikawa
Kinki University, Higashiosaka, Japan
J.S. Song, C.S. Yoon
Gyeongsang National University, Jinju, Korea
K. Kodama, N. Ushida
Aichi University of Education, Kariya, Japan
S. Aoki, T. Hara
Kobe University, Kobe, Japan
T. Delbar, D. Favart, G. Grégoire, S. Kalinin, I. Makhlioueva
Université Catholique de Louvain, Louvain-la-Neuve, Belgium
A. Artamonov, P. Gorbunov, V. Khovansky, V. Shamanov, I. Tsukerman
Institute for Theoretical and Experimental Physics, Moscow, Russian Federation
N. Bruski, D. Frekers
Westfälische Wilhelms-Universität, Münster, Germany[2]
K. Hoshino, J. Kawada, M. Komatsu, M. Miyanishi, M. Nakamura, T. Nakano, K. Narita, K. Niu, K. Niwa, N. Nonaka, O. Sato, T. Toshito
Nagoya University, Nagoya, Japan
S. Buontempo, A.G. Cocco, N. D'Ambrosio, G. De Lellis, G. De Rosa, F. Di Capua, G. Fiorillo, A. Marotta, P. Migliozzi, L. Scotto Lavina, P. Strolin, V. Tioukov
Università Federico II and INFN, Naples, Italy
T. Okusawa
Osaka City University, Osaka, Japan
U. Dore, P.F. Loverre, L. Ludovici, G. Rosa, R. Santacesaria, A. Satta, F.R. Spada
Università La Sapienza and INFN, Rome, Italy
E. Barbuto, C. Bozza, G. Grella, G. Romano, C. Sirignano, S. Sorrentino
Università di Salerno and INFN, Salerno, Italy
Y. Sato, I. Tezuka
Utsunomiya University, Utsunomiya, Japan

[1] Now at Università La Sapienza, Rome, Italy.
[2] Supported by the German Bundesministerium für Bildung und Forschung under contract numbers 05 6BU11P and 05 7MS12P.
[3] Now at SpinX Technologies, Geneva, Switzerland.
[4] Fonds voor Wetenschappelijk Onderzoek, Belgium.
[5] Fonds National de la Recherche Scientifique, Belgium.
[6] Now at DESY, Hamburg.
[7] On leave of absence and at St. Kliment Ohridski University of Sofia, Bulgaria.
[8] Now at CPPM CNRS-IN2P3, Marseille, France.
[9] On leave of absence from INFN, Ferrara, Italy.

1 Introduction

In the study of multi-particle production processes, the multiplicity of charged particles is an important global parameter reflecting the dynamics of the interaction. Different phenomenological and theoretical models can be tested and therefore multiplicities have been studied in experiments with different particle beams, making use of various techniques and over a wide range of kinematic variables.

The characteristics of charged-particle multiplicity distributions have been studied in detail in high energy hadronic collisions [1], in e^-e^+ annihilation [2, 3], and in interactions of neutrinos and anti-neutrinos on nucleons and light nuclei [4, 5, 6, 7, 8]. In particular, Bubble Chamber experiments [9, 10, 11] performed measurement of the charged particle multiplicity, produced in ν_μ ($\overline{\nu}_\mu$)n and ν_μ ($\overline{\nu}_\mu$)p interactions. They also studied the multiplicity moments as function of kinematical quantities.

The sub-micron spatial resolution of nuclear emulsion allows both the investigation of the event topology and the measurement of the angular distribution of charged particles to be performed with high accuracy. Therefore, it is well suited to study particle-production multiplicities. However, such data on neutrino interactions in nuclear emulsion are relatively scarce [12, 13] and don't exist for anti-neutrino interactions in nuclear emulsion.

In this paper, we report on a study of charged-particle multiplicities produced in high-energy charged-current (anti-)neutrino interactions in a nuclear emulsion target measured with the CHORUS hybrid detector. Such data are useful in tuning interaction models in Monte Carlo event generators. We also investigate the KNO scaling [14] behaviour in different kinematical regions.

2 The experimental apparatus

The CHORUS detector [15] is a hybrid setup that combines a nuclear emulsion target with several electronic detectors: trigger hodoscopes, a scintillating fibre tracker system, a hadron spectrometer, a calorimeter and a muon spectrometer.

The target consists of *Fuji ET-7B* [16] nuclear emulsions with properties given in Table 1. The nominal sensitivity is 30 grains per 100 μm for minimum-ionizing particles. The target is segmented into four stacks and has an overall mass of 770 kg. Each of the stacks consists of eight modules of 36 plates of size 36 cm $\times$ 72 cm. Each plate has a 90 μm plastic support coated on both sides with a 350 μm emulsion layer. Particle track directions are nearly perpendicular to the emulsion sheets. This configuration permits fast automatic scanning of the emulsion sheets.

Each target stack is followed by three interface emulsion sheets with 90 μm emulsion layers on both sides of an 800 μm thick plastic base and by a set of scintillating-fibre tracker planes [17]. The interface sheets and the fibre trackers provide accurate particle trajectory measurements which are extrapolated into the emulsion stack in order to locate the neutrino interaction vertices. The accuracy of the fibre tracker prediction is about 150 μm in the track position and 2 mrad in angle.

The electronic detectors downstream of the emulsion target include a hadron spectrometer that measures the bending of charged particles in an air-core hexagonal magnet [18], a calorimeter where the energy and direction of showers are measured and a muon spectrometer which measures the charge and the momentum of muons. The energy resolution for hadronic showers of the calorimeter is $\sigma(E)/E = (0.323 \pm 0.024)/\sqrt{E/\mathrm{GeV}} + (0.014 \pm 0.007)$ [19]. The muon spectrometer consists of six magnetized iron toroids sandwiched between seven tracking stations (drift chambers and streamer tubes). The muon momentum resolution varies from $\approx$15% in the 12–28 GeV/c range [20] to 19% at about 70 GeV/c [15], as measured with test-beam muons.

The West Area Neutrino Facility (WANF) of the CERN SPS provided an intense beam of neutrinos with an average energy of 27 GeV. The beam consisted mainly of ν_μ with a contamination of $\sim$5% $\overline{\nu}_\mu$ and $\sim$1% ν_e. The CHORUS detector was exposed to the wide band neutrino beam (section 5 of [15] for details) of the CERN SPS during the years 1994–1997, with an integrated flux of 5.06×10^{19} protons on target. In this four year exposure more than 10^6 neutrino interactions were accumulated in the emulsion target.

3 Analysis

The emulsion scanning has been performed by fully automatic microscopes each equipped with a CCD camera and a fast custom built processor (originally called 'Track Selector') [21] capable of iden-

Table 1: Atomic composition and main features of the nuclear emulsions (Fuji ET-B7) used in the CHORUS experiment [24]

Element	**Atomic number**	**Mass (%)**	**Mole fraction (%)**
Iodine (I)	53	0.3	0.06
Silver (Ag)	47	45.5	11.2
Bromine (Br)	35	33.4	11.1
Sulphur (S)	16	0.2	0.2
Oxygen (O)	8	6.8	11.3
Nitrogen (N)	7	3.1	5.9
Carbon (C)	6	9.3	20.6
Hydrogen (H)	1	1.5	40.0

Mean number of nucleons	36 protons, 45 neutrons
Density	3.73g/cm^3
Radiation length	2.94 cm
Nuclear interaction mean free path	38 cm
Concentration of AgBr	45.5% in volume

tifying tracks inside the emulsions, and measuring on-line their parameters. The track finding efficiency of the Track Selector is higher than 98% for tracks with an angle of less than 400 mrad [22] with respect to the beam direction, perpendicular to the emulsion plates.

The location of the emulsion plate containing the interaction vertex is achieved with a procedure which is called scan-back [23]. As a first step, tracks reconstructed by the electronic detectors are followed upstream into the emulsion stacks. A track, extrapolated from the fibre-trackers and found in the interface emulsion sheets, is followed upstream in the target emulsion stack using track segments reconstructed in the most upstream 100 μm of each plate. If the track is not found in two subsequent plates, the first plate with no track hit is defined as the plate containing the vertex. In total, about 150 000 ν_μ CC events with at least one reconstructed muon in spectrometer, have been located in emulsion as a result of this procedure.

For the present measurement, from the 150000 located events with at least one reconstructed muon in the spectrometer, a sample of 1208 events was randomly selected to be visually inspected and to measure the parameter associated with the charged tracks at the (anti-)neutrino vertex. We use the sign of the charge of the highest-energy muon in the events, as determined by the muon spectrometer, to determine whether the interaction was induced by a neutrino or an anti-neutrino. In order to have a larger anti-neutrino sample, events located in various modules of the emulsion stacks have been collected, while the neutrino sample consists of events located in one half module of an emulsion stack. In 627 (581) of the selected events the charge of the leading muon is negative (positive).

To evaluate the number of genuine $\overline{\nu}_\mu$ charged-current (CC) interactions, one has to subtract from this sample the contamination due to:

- ν_μ CC events with the μ^- reconstructed as a μ^+;
- punch-through hadrons traversing the 5.2 interaction lengths of the calorimeter and reconstructed as positive muons in the spectrometer. This can happen in CC events where the μ is not identified or in NC interactions;

In order to reduce this background, a set of selection criteria improving the reliability of the muon reconstruction is applied to the events with a muon reconstructed with positive charge:

- low momentum muons stopping inside the spectrometer, for which the reconstruction is based on only a few hits in the electronic detectors, are discarded;
- the impact point on the spectrometer entrance surface is required to be within a 150 cm radius centered around its axis to ensure a long potential path through the toroidal magnets;
- the track length is required to be greater than three spectrometer gaps (two magnets) and consistency checks are made among the various reconstruction algorithms;

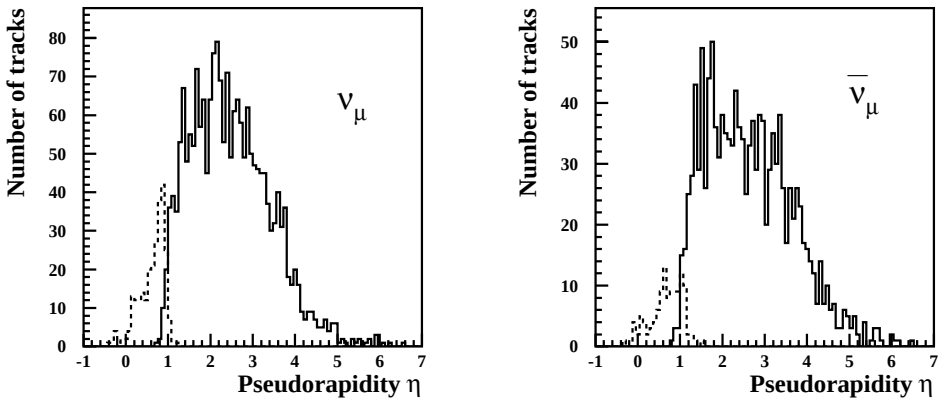

Figure 1: Pseudo-rapidity distributions for tracks classified as shower (full histogram) and grey (dashed histogram) by the scanner.

– the trajectory of the muon measured in the spectrometer is required to match with a track detected in the fibre trackers, and a selection criterion is applied on the basis of χ^2 of the global track fit.

These criteria select 529 events with a reconstructed positive muon. The contribution from π and K decays into a μ, reconstructed in the spectrometer is negligible, as well as ν_μ induced charm events with the μ^- reconstructed as a μ^+. The remaining background to the sample of μ^+ due to ν_μ events is composed of punch-through tracks of pions and kaons and amounts to 5.5 ± 1.9 (stat) ± 0.6 (syst) events.

We further require that square of the invariant mass of the hadronic system, W^2, of (anti-)neutrino events is greater than 1 GeV$^2/c^4$. After this selection the number of ν_μ–A ($\overline{\nu}_\mu$–A) interactions is 496 (369).

4 Measurement procedure and charged prong classification in nuclear emulsions

When a charged particle passes through nuclear emulsion it forms a latent image by ionizing the AgBr crystals along its trajectory. After a suitable chemical processing of the emulsions such ionization sites induce the deposition of Ag atoms as dark spots (grains) thus making the trajectory of the charged particles visible. Tracks are usually classified according to their grain density (number of Ag grains per unit length) as shower, grey and black prongs following the procedure described in Refs. [25, 26]. Shower tracks correspond to relativistic (or nearly relativistic) singly charged particles with a velocity $\beta \geq 0.7$. Their grain density is $g < 1.4\ g_0$ (g_0 represents the plateau grain density of a highly relativistic singly charged particle, which equals 29.6 grains per 100 μm for the CHORUS emulsion). Grey tracks correspond to charged particles with velocity $0.25 \leq \beta < 0.7$. They are interpreted as recoil nucleons emitted during the nuclear cascade. Their grain density is $1.4\ g_0 < g < 10\ g_0$. The black prongs correspond to particles with a velocity $\beta < 0.25$. These are produced by low energy fragments (protons, deuterons, alphas and heavier fragments) emitted from the excited target nucleus. The associated grain density is $g \geq 10\ g_0$.

The above criteria commonly used in nuclear emulsion experiments are very difficult to apply in the CHORUS analysis since the emulsion sheets were exposed perpendicular to the beam direction. Furthermore, electronic measurement of the energy and momentum for every charged particle was not possible due to geometrical acceptances.

The following procedure was used for the CHORUS data. Once the vertex plate had been located by the automatic system, the event was checked and measured extensively with a manually controlled microscope system. The black prongs at a neutrino interaction vertex, due to heavily ionizing particles, have short path lengths and usually stop within one emulsion plate so that they can be recognized. For the remaining mixture of shower and grey prongs, we measured the particle directions. These particles are mainly pions with a small contamination of protons.

Ambiguity in classifying shower and grey prongs can arise either due to the difficulty in strictly applying the ionization criteria in the manual scanning or due to variations in the quality of the optics of the microscope. To overcome these limitations we decided to classify these prongs by using the pseudo-rapidity variable [27]:

$$\eta = -\ln\tan\frac{\theta}{2} \tag{1}$$

where θ is the emission angle of the prong with respect to the neutrino direction. This has the advantage of being independent of the scanner and of the microscope optics, allowing us to compare in a straightforward manner the multiplicity measurements with the theoretical models. The pseudo-rapidity distributions for tracks classified as shower and grey by the scanner, both for neutrino and anti-neutrino interactions are shown in Fig. 1. These plots show that a scanner-independent classification, based on the pseudo-rapidity, is possible and it is consistent with the traditional one. In the following, all prongs with $\eta \geq 1$ are classified as shower particles. By applying this cut the fraction of shower (grey) tracks miss-identified as grey (shower) is (1.23±0.19)% ((7.27±1.40)%). The multiplicities of shower, grey and heavy (grey+black) prongs are denoted by $n_{\rm s}$, $n_{\rm g}$ and $n_{\rm h}$, respectively. The total number of charged hadrons classified as shower particles in an event is defined to be $n_{\rm ch} = n_{\rm s} - 1$, namely the number of shower tracks minus the muon track.

5 Efficiency Evaluation

Reconstruction and location efficiencies were evaluated making a detailed simulation of the detector response using a program based on GEANT3 [28]. Large samples of deep-inelastic neutrino interactions (DIS) were generated using the beam spectrum from the CHORUS JETTA generator [29] based on LEPTO [30] and JETSET [31]. Quasi-elastic (QE) interactions and resonance production (RES) events were generated with the RESQUE [32] package with a rate of 9.6% relative to deep-inelastic scattering reactions in the neutrino case (26% in the anti-neutrino case). The simulated response of the electronic detectors was processed through the same reconstruction program as that used for the experimental data. The location efficiency was parametrized by a function of the primary muon momentum and angle on which it depends only weakly. The reconstruction and location efficiency as a function of the invariant mass of the hadronic system W^2 and of the shower prong multiplicities $n_{\rm ch}$ is given in Tables 2 and 3 for ν–A and $\overline{\nu}$–A interactions, respectively. The samples are normalized in such a way that the efficiency at the first bin is taken as 1.00. Given the fact that Bjorken y distributions in neutrino and anti-neutrino interactions are different, the momentum distribution of the positive muon from $\overline{\nu}_\mu$ CC interactions is harder than that of the negative muon in ν_μ CC interactions. Therefore, the reconstruction and location efficiencies of $\overline{\nu}_\mu$ CC events are higher than that of ν_μ CC events. The efficiency does not depend on the black and grey track multiplicity at the primary vertex.

In ν_μ ($\overline{\nu}_\mu$) CC interactions, the full kinematics of the event can be reconstructed from the measurement of the muon momentum p_μ, the angle θ_μ of the produced muon with respect to the beam axis, and E_{had}, the energy transfer to the hadronic system:

$$E_\nu = E_\mu + E_{had}$$

$$Q^2_\nu = 2E_\nu(E_\mu - p_\mu\, cos\theta_\mu) - m^2_\mu$$

$$W^2_\nu = 2m_n(E_\nu - E_\mu) + m^2_n - Q^2_\nu$$

where E_ν and E_μ are the energy of the incoming (anti-)neutrino and (anti-)muon energy respectively, -Q^2_ν the squared four-momentum transfer, m_n and m_μ are the mass of the nucleon and muon respectively, W^2_ν is the square of the invariant mass of the hadronic system. The average neutrino energy of the neutrino sample is $\langle E_\nu \rangle$ = (38.0 ± 1.4) GeV, the mean-square momentum transferred to the hadronic system is $\langle Q^2_\nu \rangle$ = (8.6 ±0.5) $(\mathrm{GeV}/c)^2$, and the mean-square of the invariant mass of the hadronic system is W^2_ν = (26.2 ± 1.3) GeV^2/c^4. For the antineutrino sample these values are $\langle E_{\overline{\nu}} \rangle$ = (42.5 ± 1.6) GeV, $\langle Q^2_{\overline{\nu}} \rangle$ = (4.6 ± 0.3) $(\mathrm{GeV}/c)^2$, and $W^2_{\overline{\nu}}$ = (17.7 ± 0.8) GeV^2/c^4, respectively. All distributions presented hereafter include the efficiency correction.

6 Multiplicity Distributions

The hadronic shower and heavy prong multiplicity distributions based on the pseudo-rapidity selection are shown in Fig. 2 and the distribution as a function of emission angle of shower tracks is given in Table 4[1)]. The average number of shower prongs in neutrino-nucleus interactions is $\langle n_{\rm ch}(\nu\text{–A})\rangle = 3.4 \pm 0.1$. The average heavy prong multiplicity is measured to be $\langle n_{\rm h}(\nu\text{–A})\rangle = 4.7 \pm 0.2$. The average number of shower and heavy prongs in anti-neutrino induced events are measured to be $\langle n_{\rm ch}(\overline{\nu}\text{–A})\rangle = 2.8 \pm 0.1$ and $\langle n_{\rm h}(\overline{\nu}\text{–A})\rangle = 3.5 \pm 0.2$, respectively. These two quantities were never measured yet in nuclear emulsion.

The average shower prong multiplicities $n_{\rm ch}$ for ν–A and $\overline{\nu}$–A interactions are plotted as a functions of W^2 in Fig. 3. The numerical values are given in Tables 5 and 6. The mean multiplicities are in good agreement with a linear dependence on $\ln W^2$,

$$\langle n_{\rm ch}\rangle = a + b \ln W^2 \ . \tag{2}$$

This expression was fitted to the average multiplicities for W^2 between 1 GeV$^2/c^4$ and 200 GeV$^2/c^4$. The values for the fit parameters a and b were found to be

$$n_{\rm ch}(\nu\text{–A}) = (0.45 \pm 0.24) + (0.94 \pm 0.08) \ln W^2$$

$$n_{\rm ch}(\overline{\nu}\text{–A}) = (0.53 \pm 0.20) + (0.82 \pm 0.08) \ln W^2.$$

The fitted values of a and b obtained in other experiments are shown in Table 7. Our result on a disagrees with the unpublished result of [12] at two sigma level. However we note that the value of a found in Ref [12] is much larger than the corresponding value found in all other experiments.

For the first time a sample of (anti-)neutrino events measured in emulsions is large enough to study (QE+RES)-like topologies. In order to have a minimum bias sample of (QE+RES)-like events, the $W^2 \geq 1$ GeV$^2/c^4$ cut was not applied to the located events. Hence, the starting sample of ν_μ–A ($\overline{\nu}_\mu$–A) interactions becomes 627 (529). An event is defined as being (QE+RES)-like, if the number of shower prongs is zero or one and the number grey prongs zero or one for for ν–A interactions regardless of the number of black tracks. In order to obtain (QE+RES)-like enriched sample in $\overline{\nu}$–A interactions, the sum of shower prongs and grey prongs is required to be one or zero regardless of the number of black tracks. The efficiency of this selection is estimated from the MC simulation to be 72% (81%) for ν_μ–A ($\overline{\nu}_\mu$–A) interactions. In order to suppress background from DIS interactions we further require $W^2 < 10$ GeV$^2/c^4$ for both samples. After this selection the number of (QE+RES)-like events is reported in Table 8. The average values of kinematical parameters, $\langle E_\nu\rangle$, $\langle Q^2_\nu\rangle$, $\langle W^2\rangle$, corresponding to these events are given in Table 9[2)]. The number of background events that mimic (QE+RES)-like topology is obtained from the MC simulation to be 83.4 and 73.5 events for ν_μ–A and $\overline{\nu}_\mu$–A interactions respectively. The ratio of reconstruction and location efficiency of (QE+RES)-like events to that of all CC events is found to be 1.22 (1.13) for ν_μ–A ($\overline{\nu}_\mu$–A) interactions.

After applying the efficiency and background corrections, the fraction of (QE+RES)-like events is found to be (13.4$\pm$1.0$\pm$2.0)% for ν_μ and (26.3$\pm$1.4$\pm$3.9)% for $\overline{\nu}_\mu$ interactions, respectively. These values are in reasonable agreement with the ones used in the Monte Carlo simulation (Section 5). We have accounted for a systematic uncertainty of 15% coming from the efficiency and background estimation by Monte Carlo modeling.

The sub-sample of (QE+RES)-like ν_μ ($\overline{\nu}_\mu$) events with neither black nor grey prongs is important for the understanding of nuclear mechanisms involving hadrons in the nucleus. The fraction of this type of topology is measured as (1.2$\pm$ 0.4$\pm$0.2)% for ν_μ and (9.5$\pm$1.0$\pm$1.4)% for $\overline{\nu}_\mu$ interactions, respectively. For the neutrino events the proton in the final state is absorbed by the nucleus without any visible activity. On the other hand, this fraction is larger for anti-neutrinos since in the final state there is a neutron.

[1)] The corrected number of events is 1231(844) for ν_μ–A ($\overline{\nu}_\mu$–A) interactions

[2)] Due to detector resolutions, there are 62(52) events with W^2 <0 in neutrino(anti-neutrino) sample. For these events, W^2 is taken to be m_n^2.

Table 2: The reconstruction and location efficiency in ν–A as a function of the invariant mass of the hadronic system W^2 and the number of shower tracks.

W^2	$n_{\rm ch} = n_{\rm s} - 1$						
GeV$^2/c^4$	0	1	2	3	4	≥ 5	All
$1 \div 3$	1.00± 0.03	0.95± 0.01	0.98± 0.01	0.88± 0.04	0.79± 0.08	0.71± 0.43	0.96±0.01
$3 \div 6$	0.89± 0.04	0.92± 0.01	0.93± 0.01	0.88± 0.01	0.92± 0.04	0.88± 0.09	0.91±0.01
$6 \div 10$	0.85± 0.04	0.85± 0.01	0.88± 0.01	0.82± 0.01	0.80± 0.02	0.73± 0.04	0.84±0.01
$10 \div 14$	0.76± 0.07	0.77± 0.02	0.81± 0.02	0.78± 0.01	0.81± 0.02	0.73± 0.02	0.78±0.01
$14 \div 18$	0.40± 0.12	0.75± 0.02	0.76± 0.02	0.72± 0.01	0.78± 0.02	0.71± 0.02	0.74±0.01
$18 \div 24$	0.47± 0.12	0.72± 0.02	0.74± 0.02	0.71± 0.01	0.75± 0.02	0.72± 0.02	0.72±0.01
$24 \div 32$	0.31± 0.15	0.71± 0.03	0.66± 0.03	0.67± 0.01	0.71± 0.02	0.69± 0.01	0.69±0.01
$32 \div 45$	0.55± 0.24	0.67± 0.03	0.69± 0.03	0.68± 0.02	0.64± 0.02	0.66± 0.01	0.67±0.01
$45 \div 63$	0.43± 0.35	0.61± 0.05	0.58± 0.05	0.66± 0.02	0.66± 0.02	0.60± 0.01	0.62±0.01
> 63	0.77± 0.28	0.56± 0.05	0.66± 0.05	0.59± 0.02	0.62± 0.02	0.53± 0.01	0.55±0.01
All	0.91±0.01	0.86±0.01	0.86±0.01	0.74±0.01	0.73±0.01	0.63±0.01	0.75±0.01

Table 3: The reconstruction and location efficiency in $\overline{\nu}$–A as a function of the invariant mass of the hadronic system W^2 and the number of shower tracks.

W^2	$n_{\rm ch} = n_{\rm s} - 1$					
GeV$^2/c^4$	0	1	2	3	$\geq$4	All
$1 \div 4$	1.00± 0.02	0.96± 0.02	0.98± 0.02	0.99± 0.05	0.92± 0.19	0.98±0.01
$4 \div 8$	0.95± 0.03	0.95± 0.02	0.95± 0.02	0.96± 0.04	0.88± 0.06	0.94±0.01
$8 \div 14$	0.96± 0.04	0.90± 0.03	0.90± 0.02	0.99± 0.03	0.91± 0.03	0.92±0.01
$14 \div 20$	0.82± 0.07	0.67± 0.05	0.92± 0.03	0.99± 0.04	0.90± 0.03	0.92±0.01
$20 \div 28$	0.97± 0.08	0.73± 0.06	0.83± 0.04	0.88± 0.04	0.90± 0.02	0.86±0.01
$28 \div 45$	0.85± 0.09	0.79± 0.05	0.86± 0.04	0.88± 0.04	0.90± 0.02	0.87±0.01
> 45	0.74± 0.09	0.65± 0.05	0.73± 0.04	0.73± 0.03	0.67± 0.01	0.68±0.01
All	0.97± 0.01	0.90± 0.01	0.92± 0.01	0.91± 0.01	0.81 ±0.01	0.90±0.01

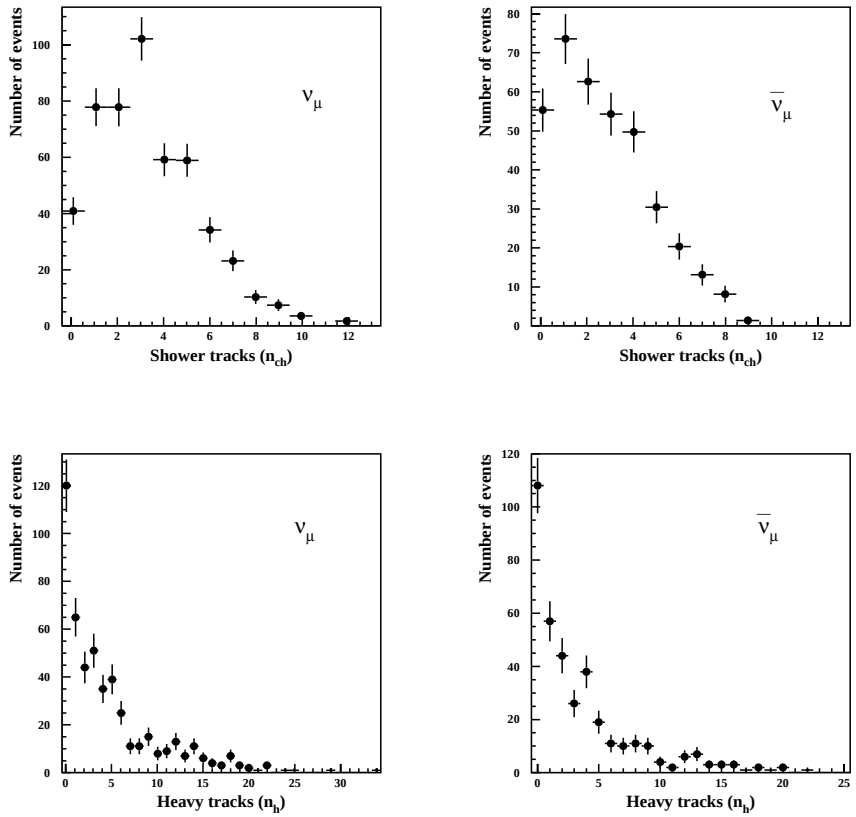

Figure 2: Multiplicity distributions for hadronic shower (top) and black plus grey (bottom) tracks in ν_μ–nucleus and $\overline{\nu}_\mu$–nucleus interactions

7 Dispersion and Koba–Nielsen–Olesen distributions

We have also investigated the dependence of the dispersion, $D_{\rm ch}$, of the shower hadron multiplicity distribution, on the average multiplicity. The dispersion $D_{\rm ch}$ is defined as

$$D_{\rm ch} \stackrel{\rm def}{=} \sqrt{\langle n_{\rm ch}^2 \rangle - \langle n_{\rm ch} \rangle^2}\ . \tag{3}$$

For independent particle production, the multiplicity follows a Poisson distribution. Therefore, one gets

$$D_{\rm ch} = \sqrt{\langle n_{\rm ch} \rangle}. \tag{4}$$

Table 4: The number of shower hadrons in ν_μ ($\overline{\nu}_\mu$) as a function of emission angle θ where $\rm N_{tr}$ is the number of hadron tracks $\frac{\rm N_{tr}}{\rm N_{ev}}$ is the ratio of the number hadrons tracks to the total number of events.

θ **(Radian)**	$\langle\theta\rangle$	$\rm N_{tr}$	$\frac{\rm N_{tr}}{\rm N_{ev}}$
$0.000 \div 0.050$	0.032±0.001 (0.031±0.001)	346 (161)	0.28(0.19)
$0.050 \div 0.100$	0.075±0.001 (0.073±0.001)	554 (282)	0.45(0.34)
$0.100 \div 0.150$	0.125±0.001 (0.123±0.001)	510 (270)	0.41(0.32)
$0.150 \div 0.200$	0.174±0.001 (0.176±0.001)	394 (280)	0.32(0.33)
$0.200 \div 0.300$	0.245±0.002 (0.246±0.002)	774 (394)	0.63(0.47)
$0.300 \div 0.400$	0.350±0.002 (0.347±0.002)	538 (330)	0.44(0.39)
$0.400 \div 0.500$	0.451±0.002 (0.449±0.003)	380 (278)	0.31(0.33)
$0.500 \div 0.600$	0.544±0.003 (0.544±0.003)	290 (171)	0.24(0.20)
> 0.600	0.651±0.003 (0.655±0.004)	210 (121)	0.17(0.15)

Table 5: The shower multiplicity distributions in ν–A as a function of W^2 (errors shown are statistical only).

W^2 GeV$^2/c^4$	$\langle W^2 \rangle$ GeV$^2/c^4$	$\langle n_{\rm ch} \rangle$	$\langle n_{\rm g} \rangle$	$n_{\rm ch} = n_{\rm s} -$ muon												**Events**
				0	1	2	3	4	5	6	7	8	9	10	$\geq$11	
$1 \div 3$	1.95±0.07	1.39±0.19	4.39±0.64	21	17	15	3	2	1	1	1	0	0	0	0	61
$3 \div 6$	4.18±0.11	2.21±0.27	5.80±0.93	10	12	12	10	5	1	2	0	0	2	0	0	54
$6 \div 10$	7.89±0.14	2.08±0.19	3.76±0.59	9	17	10	18	4	1	2	0	0	0	0	0	61
$10 \div 14$	12.09±0.18	2.86±0.29	3.28±0.61	3	13	12	7	6	4	2	2	0	0	1	0	50
$14 \div 18$	15.88±0.18	3.22±0.26	4.42±0.67	3	10	7	13	6	6	5	3	0	0	0	0	53
$18 \div 24$	21.22±0.23	3.63±0.26	4.18±0.71	1	5	6	19	5	6	4	5	1	0	0	0	52
$24 \div 32$	27.37±0.32	3.37±0.21	3.38±0.57	0	6	11	12	10	8	5	1	0	0	0	0	53
$32 \div 45$	37.36±0.59	3.67±0.34	3.10±0.69	1	4	6	6	6	6	2	2	2	0	0	0	35
$45 \div 63$	52.26±0.32	4.43±0.36	5.13±0.89	0	2	6	7	9	7	2	2	2	1	0	1	39
> 63	112.50±7.78	4.95±0.36	3.43±0.53	0	2	3	5	4	12	4	2	3	2	1	0	38
Total																496

Table 6: The shower multiplicity distributions in $\overline{\nu}$–A as a function of W^2 (errors shown are statistical only).

W^2 GeV$^2/c^4$	$\langle W^2 \rangle$ GeV$^2/c^4$	$\langle n_{\rm ch} \rangle$	$\langle n_{\rm g} \rangle$	$n_{\rm ch} = n_{\rm s} -$ muon										**Events**
				0	1	2	3	4	5	6	7	8	≥ 9	
$1 \div 4$	2.06±0.10	1.02±0.17	3.53±0.51	31	21	5	3	3	1	1	0	0	0	65
$4 \div 8$	5.84±0.14	1.94±0.20	3.21±0.48	15	13	15	9	10	2	0	0	1	0	65
$8 \div 14$	11.38±0.24	2.58±0.22	4.25±0.65	5	12	15	11	9	3	0	3	0	0	58
$14 \div 20$	16.65±0.22	2.96±0.26	2.99±0.54	3	11	13	10	3	4	8	1	0	0	53
$20 \div 28$	23.97±0.30	3.04±0.31	3.24±0.55	4	9	12	9	4	5	3	3	1	1	51
$28 \div 45$	35.06±0.72	3.89±0.29	2.42±0.49	2	4	4	8	10	8	4	3	2	0	45
> 45	87.73±8.34	3.73±0.35	2.87±0.71	1	5	1	6	9	5	2	1	2	0	32
Total														369

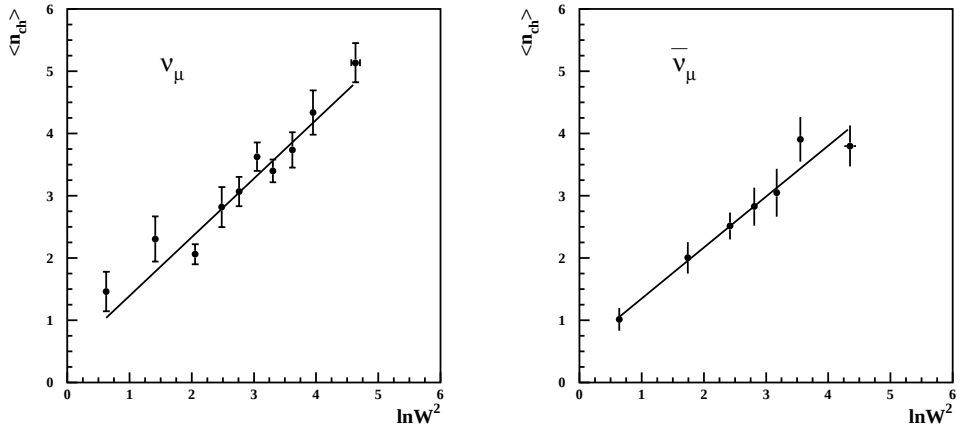

Figure 3: The hadronic shower prong multiplicity distributions as a function of $\ln W^2$ for ν–A, and $\overline{\nu}$–A interactions.

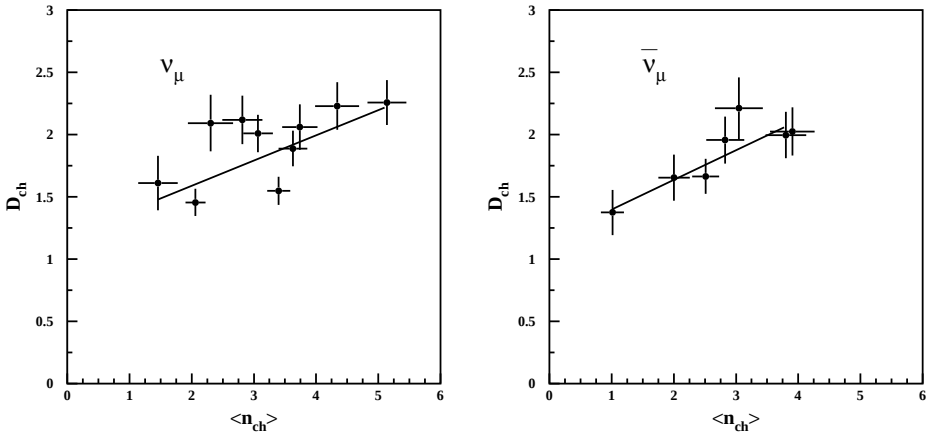

Figure 4: The hadronic shower prong multiplicity dispersion as a function of $\langle n_{\rm ch}\rangle$ for ν–A and $\overline{\nu}$–A interactions.

For charged particle production in hadronic interactions, however, an empirical relation [33] was found

$$D_{\rm ch} = A + B\langle n_{\rm ch}\rangle \, . \tag{5}$$

The linear dependence of the $D_{\rm ch}$ on $\langle n_{\rm ch}\rangle$ would imply that the shape of the distribution of the normalized multiplicity is independent of the hadronic effective mass W. Koba, Nielsen and Olesen have shown that at asymptotically high energies, a probability $P(n_{\rm ch})$ to produce an interaction of multiplicity $n_{\rm ch}$ scaled by the average $\langle n_{\rm ch}\rangle$ is independent of the energy.

$$\langle n_{\rm ch}\rangle \cdot P(n_{\rm ch}) \stackrel{E\to\infty}{\longrightarrow} \Psi\left(z = \frac{n_{\rm ch}}{\langle n_{\rm ch}\rangle}\right) \, , \tag{6}$$

where Ψ is the probability distribution independent of energy. This is called Koba-Nielsen-Olesen (KNO) scaling. Exact KNO-scaling demands that, in the linear dependence of the dispersion on the average multiplicity, Eq. 5, the intercept parameter A is exactly equal to zero. For our event samples, $D_{\rm ch}$ is given as a function of $\langle n_{\rm ch}\rangle$ in Fig. 4 with a linear fit superimposed. The values of the fit parameters are

$$D_{\rm ch}(\nu\text{–A}) = (1.18 \pm 0.17) + (0.20 \pm 0.05)\langle n_{\rm ch}\rangle$$

$$D_{\rm ch}(\overline{\nu}\text{–A}) = (1.16 \pm 0.21) + (0.24 \pm 0.08)\langle n_{\rm ch}\rangle$$

The fitted values of A and B obtained in this and other experiments are shown in Table 10. One can observe that our data, as well as freon data, are not compatible with $A = 0$. Indeed, $A = 0$ is expected

Table 7: The values of the parameters a and b obtained by fitting the relation $n_{\rm ch} = a + b \ln W^2$ to the average charged hadron multiplicity $n_{\rm ch}$. The results of other neutrino experiments are shown for comparison. 'Em' stands for nuclear emulsion; $\langle n_+ \rangle$ and $\langle n_- \rangle$ are the mean multiplicities of positively and negative charged particles.

Reaction	E_ν **(GeV)**	**a**	**b**	**Ref.**
ν_μ– Em	40	0.45 ± 0.24	0.94 ± 0.08	This paper
ν_μ– Em	50	1.92± 0.68	1.19± 0.23	[12]
ν_μ– Em	8.7	1.07 ± 0.05	1.32±0.11	[13]
ν_μ– p	-	0.37 ± 0.02	1.33 ± 0.02	[4]
ν – Freon(CF_3Br)				
$\langle n_+ \rangle$	6	0.15 ± 0.09	0.84± 0.05	[9]
$\langle n_- \rangle$	6	-0.49 ± 0.06	0.63 ± 0.04	[9]
$\overline{\nu}_\mu$– Em	40	0.53 ± 0.20	0.82 ± 0.08	This paper
$\overline{\nu}_\mu$– p	-	0.06 ± 0.06	1.22 ± 0.03	[10]
$\overline{\nu}_\mu$– Freon				
$\langle n_+ \rangle$	6	-0.26 ± 0.20	0.56± 0.12	[9]
$\langle n_- \rangle$	6	0.16 ± 0.20	0.52 ± 0.11	[9]
$\overline{\nu}_\mu$– n	-	0.80 ± 0.09	0.95± 0.04	[11]
$\overline{\nu}_\mu$– p	-	0.02 ± 0.20	1.28 ± 0.08	[11]

Table 8: (QE+RES)-like events in ν–A and $\overline{\nu}$–A interactions.

	$n_{\rm g}$	0	1	**Total**
ν_μ	$n_{\rm ch}$ = 0	39	39	78
ν_μ	$n_{\rm ch}$ = 1	56	23	79
$\overline{\nu}_\mu$	$n_{\rm ch}$ = 0	132	25	157
$\overline{\nu}_\mu$	$n_{\rm ch}$ = 1	44		44

only for a proton or neutron target. A non zero value of A is due to the heavy nuclear targets in nuclear emulsions. In such a case one introduces a new variable z' defined as [9]

$$z' = \frac{n_{\rm ch} - \alpha}{\langle n_{\rm ch} - \alpha \rangle}. \tag{7}$$

Here $\alpha = -\langle n_0 \rangle$ and $\langle n_0 \rangle$ is the extrapolated point where the fitted dispersion line crosses the

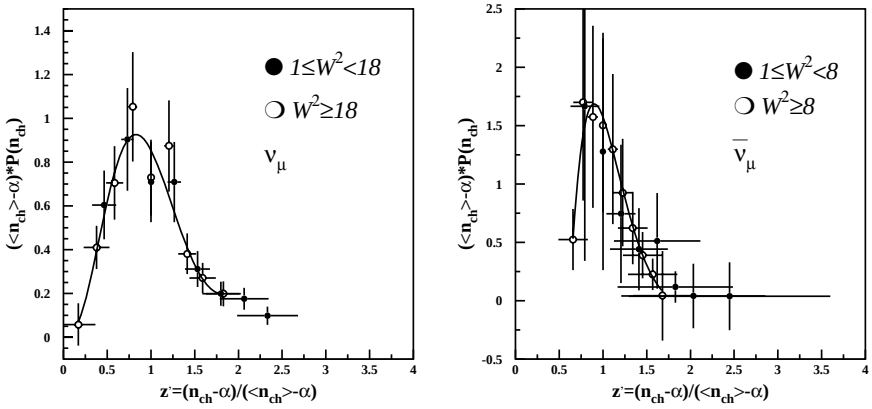

Figure 5: The KNO scaling distribution for shower prongs. The superimposed curve represents a fit to pp data [34]. The data approximately agree with KNO scaling, i.e., the data points at different W^2 intervals lie approximately on a single curve.

Table 9: Kinematic variables for (QE+RES)-like events for ν_μ and $\overline{\nu}_\mu$.

	$\langle E_\nu \rangle$ (GeV)	$\langle W^2 \rangle$ (GeV$^2/c^4$)	$\langle Q^2 \rangle$ ((GeV/c)^2)
ν_μ $n_{\rm ch}$ = 0, $n_{\rm g}$ = 0	21.7 $\pm$ 2.2	1.9 $\pm$ 0.3	0.8 $\pm$ 0.1
ν_μ $n_{\rm ch}$ = 0, $n_{\rm g}$ = 1	21.2 $\pm$ 1.9	2.6 $\pm$ 0.4	1.4 $\pm$ 0.2
ν_μ $n_{\rm ch}$ = 1, $n_{\rm g}$ = 0	21.7 $\pm$ 2.0	2.9 $\pm$ 0.4	1.5 $\pm$ 0.2
ν_μ $n_{\rm ch}$ = 1, $n_{\rm g}$ = 1	23.2 $\pm$ 2.7	3.1 $\pm$ 0.6	2.4 $\pm$ 0.3
$\overline{\nu}_\mu$ $n_{\rm ch}$ = 0, $n_{\rm g}$ = 0	21.9 $\pm$ 2.2	1.9 $\pm$ 0.3	0.8 $\pm$ 0.1
$\overline{\nu}_\mu$ $n_{\rm ch}$ = 0, $n_{\rm g}$ = 1	21.8 $\pm$ 2.0	2.4 $\pm$ 0.4	1.4 $\pm$ 0.2
$\overline{\nu}_\mu$ $n_{\rm ch}$ = 1, $n_{\rm g}$ = 0	21.1 $\pm$ 2.0	3.8 $\pm$ 0.4	1.6 $\pm$ 0.2

Table 10: Parameters of the linear fit to the dispersion distributions. The results of other neutrino experiments are also shown. Note that D_+ and D_- are the dispersion for positive and negative charged particles of reaction ν–A and $\overline{\nu}$–A, respectively.

Reaction	**A**	**B**	**Ref.**
ν_μ– Em	1.18 $\pm$ 0.17	0.20 $\pm$0.05	This paper
ν_μ– p	0.36 $\pm$ 0.03	0.36 $\pm$0.03	[4]
ν_μ– Freon			[9]
D_+	0.29 $\pm$ 0.12	0.36$\pm$0.06	
D_-	0.33 $\pm$ 0.03	0.50 $\pm$0.05	
$\overline{\nu}_\mu$– Em	1.16 $\pm$ 0.21	0.24 $\pm$0.08	This paper
$\overline{\nu}_\mu$– Freon			[9]
D_+	0.30 $\pm$ 0.11	0.64$\pm$0.20	
D_-	0.35 $\pm$ 0.04	0.35 $\pm$0.06	
$\overline{\nu}_\mu$– n	-0.10 $\pm$ 0.04	0.42$\pm$0.02	[11]
$\overline{\nu}_\mu$– p	0.28 $\pm$ 0.06	0.36$\pm$0.04	[11]

average multiplicity axis and found to be -5.82 and -4.83 for ν–A and $\overline{\nu}$–A interactions, respectively. The KNO-scaling law now reads

$$K' = (\langle n_{\rm ch} \rangle - \alpha) P(n_{\rm ch}) = \Psi(z'). \tag{8}$$

Clearly, in the asymptotic limit it makes no difference whether one uses z or z'; in fact this expression describes an approach to restore KNO scaling. Figure 5 shows the distributions obtained for $\Psi(z')$ as a function of z' for two intervals of W^2, for ν–A and $\overline{\nu}$–A samples; they are compatible with KNO scaling. Similar results have been obtained in other experiments [35, 36, 37], however, with different values of α.

8 Conclusion

The multiplicity features of (anti-)neutrino–nucleus interactions in emulsion have been investigated. The results presented in this paper have been obtained with the main objective to aid in tuning (anti-)neutrino–nucleus interaction models of the Monte Carlo event generators. To ease the use of these results, the numbers are presented in detail in the form of tables. The results can be summarized as follows.

For the first time with nuclear emulsion, the charged particle (shower, grey, black tracks) production at the neutrino interaction vertex of (QE+RES)-like events has been studied. It has been found that in (1.2+-0.4+-0.2)only the muon track is seen in the final state. These interactions are mainly from the reaction $\nu_\mu n \rightarrow \mu^- p$ and the proton is absorbed by the nucleus without any visible recoil. We also report the first study of anti-neutrino induced events in nuclear emulsion for the production of charged particles. The average number of shower and heavy prongs in anti-neutrino induced events are measured to be $\langle n_{\rm ch}(\overline{\nu}\text{–A}) \rangle = 2.8 \pm 0.1$ and $\langle n_{\rm h}(\overline{\nu}\text{–A}) \rangle = 3.5 \pm 0.2$, respectively. The fraction of (QE+RES)-like events in anti-neutrino interactions is found to be (26.3$\pm$1.4$\pm$3.9)%.

The dependence of the average multiplicity $\langle n_{\rm ch} \rangle$ on $\ln W^2$ for ν–A and $\overline{\nu}$–A interactions is compatible with being linear with similar slopes. The dispersion $D_{\rm ch}$ of the multiplicity distribution shows a linear dependence on mean multiplicity $\langle n_{\rm ch} \rangle$. The emulsion data are consistent with the KNO scaling as a function of an appropriate multiplicity variable z'.

Acknowledgements

We gratefully acknowledge the help and support of the neutrino beam staff and of the numerous technical collaborators who contributed to the detector construction, operation, emulsion pouring, development, and scanning. The experiment has been made possible by grants from the Institut Interuniversitaire des Sciences Nucléaires and the Interuniversitair Instituut voor Kernwetenschappen (Belgium), the Israel Science Foundation (grant 328/94) and the Technion Vice President Fund for the Promotion of Research (Israel), CERN (Geneva, Switzerland), the German Bundesministerium für Bildung und Forschung (Germany), the Institute of Theoretical and Experimental Physics (Moscow, Russia), the Istituto Nazionale di Fisica Nucleare (Italy), the Promotion and Mutual Aid Corporation for Private Schools of Japan and Japan Society for the Promotion of Science (Japan), the Korea Research Foundation Grant (KRF-2003-005-C00014) (Republic of Korea), the Foundation for Fundamental Research on Matter FOM and the National Scientific Research Organization NWO (The Netherlands), and the Scientific and Technical Research Council of Turkey (Turkey). We gratefully acknowledge their support.

References

[1] K.J. Biebl *et al.*, Fortschr. Phys. **V28**, 124 (1980); G.J. Alner *et al.*, Phys. Reports **154**, 245 (1987); R.E. Ansorge *et al.*, Z. Phys. **C43**, 357, (1989).
[2] C. Berger *et al.*, PLUTO Coll., Phys. Lett. **B78**, 176 (1978).
[3] W. Brandelik *et al.*, TASSO Coll., Phys. Lett. **B89**, 418 (1980).
[4] P. Allen *et al.*, Nucl. Phys. **B181**, 385 (1981).
[5] J. Bell *et al.*, Phys. Rev. **D19**, 1 (1979).
[6] G.T. Jones *et al.*, Z.Phys. **C54**, 45, (1992).
[7] H. Grässler *et al.*, Nucl. Phys. **B223**, 269 (1983).
[8] D. Zieminska *et al.*, Phys. Rev. **D27**, 47 (1983).
[9] D. S. Baranov *et al.*, Z. Phys. **C21**, 189 (1984).
[10] M. Derrick *et al.*, Phys. Rev. **D17**, 1 (1978).
[11] S. Barlag *et al.*, Z. Phys. **C11**, 283 (1982).
[12] L. Voyvodik *et al.*, ITEP-86-91, Moscow (1986).
[13] Yu. D. Aleshin *et al.*, Zh. Eksp. Teor. Fiz. **110**, 391 (1996); JTEP **83**, 208 (1996).
[14] F. Koba, H. B. Nielsen, P. Olesen, Nucl. Phys. **B40**, 317 (1972).
[15] E. Eskut *et al*, CHORUS Coll., Nucl. Instrum. Methods **A401**, 7 (1997).
[16] S. Aoki *et al*, CHORUS Coll., Nucl. Instrum. Methods **A447**, 361 (2000).
[17] P. Annis *et al.*, Nucl. Instrum. and Methods **A412**, 19 (1998).
[18] F. Bergsma *et al.*, Nucl. Instrum. and Methods **A357**, 243 (1995).
[19] S. Buontempo *et al*, CHORUS Coll., Nucl. Instrum. Methods **A349**, 70 (1994).
[20] A. Artamonov and P. Gorbunov, CHORUS Internal Note 97029, 23 February 1998, updated 12 March 1999. `http://choruswww.cern.ch/Publications/Notes/spec1mu_new.pdf`
[21] T. Nakano, Ph. D. Thesis, Nagoya University, Japan (1997).
[22] M. Güler, Ph.D. Thesis, METU, Ankara, Turkey (2000).
[23] U. Köse, Ph.D. Thesis, METU, Ankara, Turkey (2006).
[24] K. Niwa, Contrib. to the "Conference on Particle and Nuclear Astrophysics and Cosmology in the next Millennium", Snowmass (1994).
[25] C. F. Powell, P. H. Fowler and D. H. Perkins, "The Study of Elementary Particles by the Photographic Method", Pergamon Press, London (1959).
[26] W. H. Barkas, "Nuclear Research Emulsions", Volume I, II Academic Press, London (1963).
[27] F. Liu and J. Sun, Nuovo Cimento **110A**, 775 (1997).
[28] GEANT 3.21, CERN program library long write up W5013.

[29] P. Zucchelli, Ph.D. Thesis, Universitá di Ferrara, Italy (1995).
[30] G. Ingelman, *Preprint TSL/ISV* 92-0065, Uppsala University, Sweden (1992).
[31] T. Sjöstrand, *Comput. Phys. Commun.* **82**, 74 (1994).
[32] S. Ricciardi, Ph.D. Thesis, Universitá di Ferrara, Italy (1996).
[33] A. Wroblewski, Acta Phys. Polon. **B4**, 857 (1973).
[34] P. Slattery, Phys. Rev. **D7**, 2073 (1973).
[35] J. Hebert *et al.*, Phys. Rev. **D15**, 1867 (1977).
[36] J. Hebert *et al.*, Phys. Lett. **B48**, 467 (1974).
[37] R. K. Shivpuri and V. K. Verma, Z. Phys. **C58**, 7 (1993).